Annals of Biomedical Engineering, Vol. 33, No. 12, December 2005 (© 2005) pp. 1743–1751
DOI: 10.1007/s10439-005-7257-7

On the Passive Cardiac Conductivity

JEROEN G. STINSTRA,[1,2] BRUCE HOPENFELD,[4] and ROB S. MACLEOD[1,2,3]

[1]Scientific Computing and Imaging Institute, University of Utah, Salt Lake City, UT; [2]Cardio Vascular Research and Training Institute, University of Utah, Salt Lake City, UT; [3]Department of Bioengineering, University of Utah, Salt Lake City, UT; and [4]National Heart Lung and Blood Institute, NIH, Bethesda, MD

(Received 15 May 2005; accepted 7 July 2005)

Abstract—In order to relate the structure of cardiac tissue to its passive electrical conductivity, we created a geometrical model of cardiac tissue on a cellular scale that encompassed myocytes, capillaries, and the interstitial space that surrounds them. A special mesh generator was developed for this model to create realistically shaped myocytes and interstitial space with a controled degree of variation included in each model. In order to derive the effective conductivities, we used a finite element model to compute the currents flowing through the intracellular and extracellular space due to an externally applied electrical field. The product of these computations were the effective conductivity tensors for the intracellular and extracellular spaces. The simulations of bidomain conductivities for healthy tissue resulted in an effective intracellular conductivity of 0.16 S/m (longitudinal) and 0.005 S/m (transverse) and an effective extracellular conductivity of 0.21 S/m (longitudinal) and 0.06 S/m (transverse). The latter values are within the range of measured values reported in literature. Furthermore, we anticipate that this method can be used to simulate pathological conditions for which measured data is far more sparse.

Keywords—Conductivity, Cardiac tissue, Bidomain, Cardiac modeling.

INTRODUCTION

Simulation is an attractive approach for dealing with the many experimental hurdles in determining electrical conductivity of myocardial tissue. Moreover, a comprehensive simulation model could provide conductivity values under a range of physiological and pathophysiological conditions that would be impossible to determine accurately by experimental methods. The importance of electrical conductive properties lies in the well-known influence they exert not only on the process of activation spreading from cell to cell but also on the way an embedded cardiac source generates currents within the surrounding myocardium. Johnston and Kilpatrick have recently provided an illustrative example of the influence of electrical conductivity,[17] by showing in their simulations that three different sets of conductivity values cited in the literature led to significantly different epicardial potentials in otherwise identical models. These experimentally determined myocardial conductivity values vary over a two-to threefold range, largely because of the complexity—and thus uncertainty—of the measurements and the variable conditions under which each was carried out. Another reason for variation is that the effective conductivity depends on the direction, the uniformity, the frequency, and the strength of the applied current. Even if one deals adequately with the problems of measurement, conductivity also depends on many physiological parameters that vary over a range of circumstances. These parameters include the intracellular and interstitial volumes, the amount of blood flowing through the cardiac vasculature, the ionic composition of the intracellular and extracellular electrolytes, and the geometry of the myocytes. Hence, there is no single value for cardiac conductivity, and the myocardial conductivity changes throughout the heart as a function of the underlying physiology.

Another specific motivation for creating a model of myocardial conductivity was a project to simulate myocardial ischemia in a whole canine heart.[14,15] For such simulations we used the bidomain approach,[12] which requires intracellular and extracellular anisotropic conductivity tensors under normal conditions and under the varied influences of acute ischemia (e.g. differences in cell and capillary volumes due to accumulation of metabolic waste products and changes in the osmotic/hydrostatic pressure, as well as changes in gap junction conductivity and the rise in extracellular potassium), conditions for which there is very sparse experimental literature.

The overall structure of the model is a three-dimensional matrix of realistically shaped myocytes organized into fibers within an interstitial space and connected with gap junctions. We selected the size of the model (64 myocytes) and the resolution of its constitutive computational elements (about 2 μm in resolution) to capture realistically the response of a macroscopic piece of myocardium with its

Address correspondence to J. Stinstra, Nora Eccles Harrison Cardio Vascular Research and Training Institute, University of Utah, Room 207, 95 South 2000 East, Salt Lake City, UT 84112-5000. Electronic mail: jeroen@cvrti.utah.edu

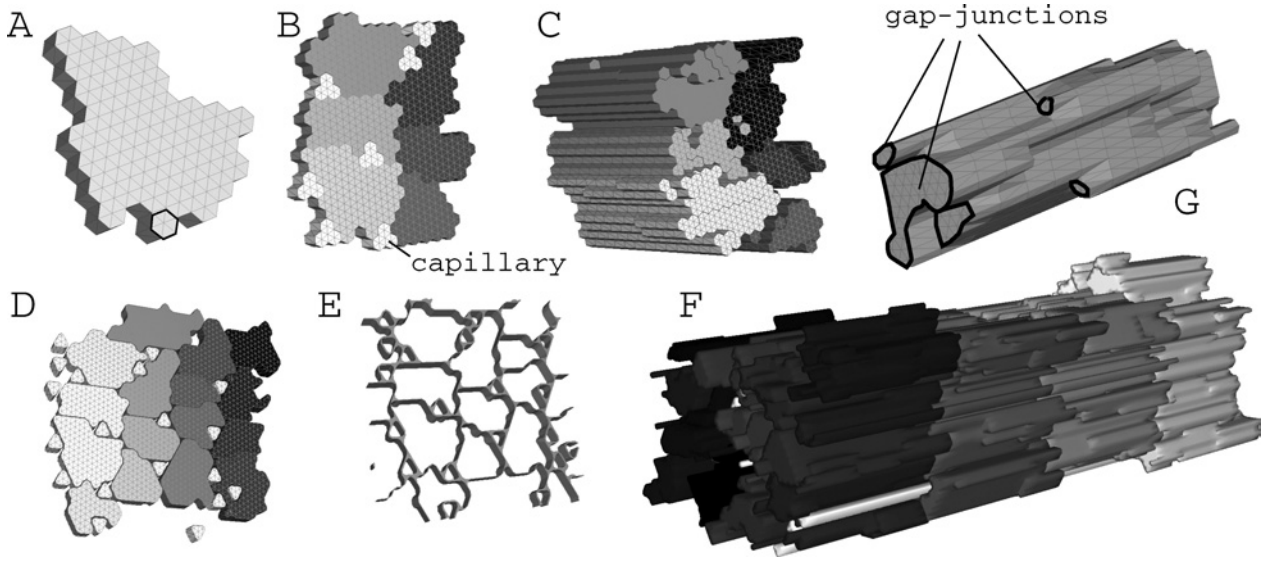

FIGURE 1. Illustration of constructing a geometric model for a piece of cardiac tissue: (A) A cross section of a myocyte created from hexagonal building blocks; (B) Several of these cross sections combined to fill a transverse plane; (C) The extrusion of the cross section into a three-dimensional matrix of cells; (D) Cross section of the smoothed model after carving out extracellular space around the cells and capillaries; (E) The extracellular mesh that surrounds all myocytes and capillaries; (F) The full three-dimensional model with separate myocytes shaded differently; (G) The arrangement of gap junctions associated with a single myocyte.

anisotropic features but without the influence of relatively larger structures such as cleavage planes,[13] changing fiber directions and features such as vasculature larger than capillaries. Using this geometrical model, we could apply an external electric field and compute the associated bulk conductivity of both the intracellular and extracellular spaces in both the longitudinal and transverse directions (σ_{il}, σ_{it} for intracellular values and σ_{el} and σ_{et} for extracellular). In accordance with the common quasi-static assumptions,[25] we computed these values under DC conditions. In addition, we assumed that no current crossed the cell membrane—the membrane had a conductivity value of zero, which allowed a separation of intracellular and extracellular conductivity, a basic assumption of the bidomain approach, where the membrane currents (both active and passive) are modeled separately.

With this model and the associated assumptions, we were able to compute all the bidomain conductivities and compare them to the values in the literature. Moreover, we were able to derive from these simulations insight regarding the extent to which the bidomain conductivities depend on the heterogeneity of morphology associated with real myocardial tissue under normal and ischemic conditions.

METHODS

Tissue Model

The model we developed consisted of two domains, the intracellular space (ICS) of the myocytes and the extracellular space (ECS) surrounding the myocytes, separated by the cell membrane. The ECS contained compartments for the interstitial electrolyte and the capillaries and the ICS domain consisted of the intracellular electrolyte and gap junctions connecting the myocytes. The fluids that filled both compartments were electrically homogenous and ohmic. Each myocyte in the model had dimensions of approximately $10\,\mu m \times 25\,\mu m \times 100\,\mu m$ and all myocytes shared the same direction of the long axis, i.e. the anisotropy was uniform.

A major goal in creating the model was to achieve not just realistic rendering of a single set of cells but to gain the ability to easily create many models that differed in ways that would capture some of the known variations in tissue structure. Thus, the model had to contain elements that could vary randomly from case to case based on average values and their standard deviations, parameters we could set based on literature values. In this way, we could also generate models that mimicked different pathophysiologies, for example, the shifts in liquid between ICS and ECS or the collapse of capillaries that occur following ischemia or the reduction in gap junctional conductivity that results from drop in pH or intracellular elevations in Ca^{2+}.

Figure 1 provides an overview of how we created the three-dimensional models of myocardium. The construction started with a slice of hexagonal elements that represented a cross section through a piece of myocardium perpendicular to the local fiber direction (Panel A). Within the slice, we seeded elements that would grow to form myocytes (shaded cells in Panel B) and also groups of three

elements that would form the capillaries (white cells in Panel B). Capillary distribution was random but approximately uniform with the density determined by a "filling factor," a parameter available from the literature.[10] Literature values also drove the algorithm that grew the myocytes but here too, there was a degree of randomness that resulted in myocytes of approximately regular pattern but varying shape. Another special feature of the model was that it generated modules of myocytes, building blocks, that could fit together perfectly to form larger pieces of tissue. To achieve the required regularity in cross section, cells that reached the edge of the original slice wrapped around to grow into the opposite edge. When the myocyte growth was completed, we moved cells from one edge to the other in order to create contiguous myocytes and the resulting irregular lateral borders visible in Panel D in the figure. The next step was to extrude the hexagonal slice to create a three-dimensional slab of myocytes separated by realistic extracellular gaps. Two parameters (mean values with random perturbations) controlled this extrusion process, one that determined myocyte length and one that determined the length of individual hexagonal tubes within each myocyte. The result was a module that was 1 cell in length, 16 cells in cross section, with the irregular end profile typical of real myocytes (Panel C in Fig. 1). In our studies, we varied myocyte length from 60 to 140 μm[26] with a mean of 100 μm and varied the cross-sectional area from 300 to 600 μm^2 with a mean of 290 μm^2.[11] Both ends of these modules were also matched so that they would stack on top of each other perfectly like building blocks (Panel F). To reflect published results of myocardial ultrastructure,[1] capillaries run parallel to the fiber direction through the entire tissue.

Histological data in the literature suggest that the ECS at the junctions of multiple myocytes is larger than when only two myocytes abut;[1] similarly, there is wider spacing between capillaries and neighboring myocytes, conditions that we mimicked in the model. Panels C and D in Fig. 1 illustrate the resulting cross sections after the ECS has been carved out in this manner with spacing between myocytes set to 0.5 μm and around capillaries set to 1 μm. To simulate the conductivity of the capillaries, we filled the volume within the endothelium with a 50% mixture of conductive blood serum and essentially insulating red blood cells.[33]

Gap junctions are a critical component of conduction in the myocardium and we included resistive connections between neighboring myocytes to recreate them in the model. In order to create an automated scheme, we assigned gap junctions to all surfaces between myocytes that were oriented perpendicularly to the fiber direction to create longitudinal connections. In order to also achieve some lateral coupling between myocytes, we altered the lateral boundaries between them to have some irregularity, as shown in Fig. 2. These irregularities produced small segments of the boundary that were perpendicular to the fiber, resulting in lateral connectivity between cells. The figure also shows the coupling at the end of myocytes in the model that allowed effective lateral connection between neighboring myocytes by means of an upstream cell that couples at the ends of both. The resulting distribution of gap junctions was 80% between the ends of the cells and rest distributed laterally, to agree with values published by Spach *et al*.[31]

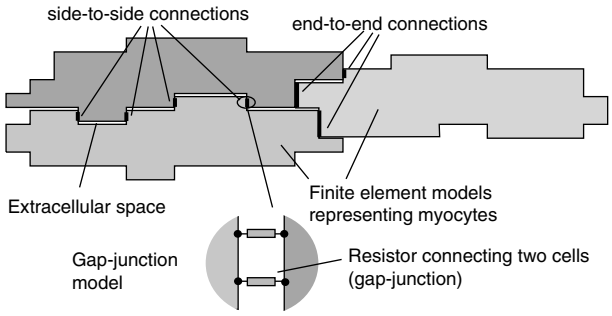

FIGURE 2. An illustration of the intracellular model and the distribution of gap junctions that connect the different myocytes in the model. By varying the shape of the myocytes along the fiber axis, both side-to-side and end-to-end connections are formed.

Because the model was constructed using elements in the micrometer range, we did not simulate individual gap junctions, but assumed an effective surface resistance for those surfaces in the model where gap junctions connect two neighboring myocytes.

Computational Mesh

The hexagonally based scheme that was the basis for constructing the model required further refinement to create a suitable polygonal mesh for the computation of conductivity. The first step involved filling the interior of each hexagonal cell with 24 tetrahedral elements using rule-based decomposition. The extracellular space could become fairly complex and we first filled this region with a combination of small prism and hexahedral elements and then further decomposed these into even smaller tetrahedra that were suitable for finite element computation. The resulting geometric model consisted of about 1.4 million elements in the ECS and 600,000 elements in the ICS.

Computing the Effective Conductivity

We computed the effective bidomain conductivities, σ_{il}, σ_{it}, σ_{el}, and σ_{et}, by applying an electrical field (E_{app}) in either the longitudinal or transverse direction across the ICS or the ECS. From the resulting net current density, we defined the bidomain conductivity to be $\sigma_e = J_{ECS}/E_{app}$, and $\sigma_i = J_{ICS}/E_{app}$. The computations assumed that there was

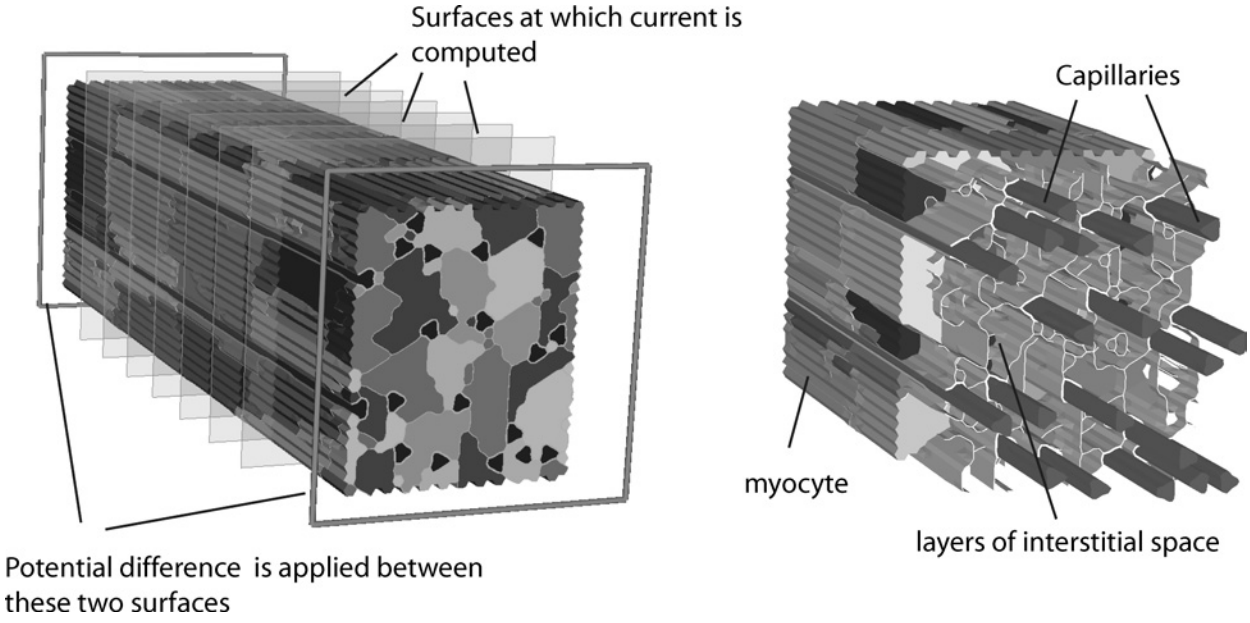

FIGURE 3. An illustration of the full conductivity model. On the left a tissue piece is shown of 4 × 4 × 4 myocytes. Each myocyte is depicted in a different color showing how they fit together to form one piece of tissue. The left panel shows as well the planes between which a voltage difference of 1 V is applied and the locations at which the current flowing through the intracellular and extracellular space was computed. The right panel displays the different components of the model, in red the distribution of capillaries is shown, and in grey the sheets of interstitial fluid are shown that surround capillaries and myocytes.

no current flow between ICS and ECS, a premise supported by experimental results.[18]

To deal with small-scale variation in conductivity we used a cluster of at least $4 \times 4 \times 4$ myocytes in order to compute reliable bulk conductivities. To prevent edge effects from even this number of myocytes from skewing the simulation results, we coupled opposite edges in the model electrically by means of the following boundary conditions: (1) A current exiting at one boundary node entered the model at the opposite boundary node; and (2) the potential at a node of the boundary was set equal to the potential of its counterpart on the opposite boundary. The latter boundary condition was modified for node pairs that align with the externally applied electrical field. The electrical field was applied by requiring that the potential difference between nodes at the opposite boundary is a constant potential drop defined by strength of electrical field multiplied by the distance traveled along the electrical field. Application of these boundary conditions allowed us to simulate an infinite slab of tissue by computing the potential distribution from just one cluster of cells.

Computing the current density within the ICS and the ECS required solving Laplace's equation separately in both volumes with the proper boundary conditions. We used the finite-element method to compute the potential distribution in both domains assuming linearly interpolated tetrahedral elements. An iterative solver determined the potentials at each node, from which we computed the potential gradient and multiplied it by the local conductivity of the interstitial and cytosolic electrolytes (described later) to derive the current density.

In order to estimate the effect of the natural variation in shape and size of myocytes, we repeated the computation of the effective conductivity for 10 different (randomly generated) clusters of cells and computed the maximum, minimum, and mean values.

Figure 3 depicts the the location where the voltage difference is applied and where the surfaces at which the current is measured. In order to compute the effective conductivity we computed the total current through seven cross-sectional planes and we used the averaged value to compute the effective conductivity value. The figure depicts the procedure to compute the longitudinal conductivity, a similar procedure was used to compute the conductivity in the transverse direction. The right panel of Fig. 3 illustrates how the extracellular space wraps around the capillaries and forms sheets of interstitial fluid between the different myocytes.

ICS and ECS Electrolyte Conductivities

The computation of the effective conductivity values required us to set realistic conductivity values for the intracellular and extracellular fluids that filled those volume. A common value for interstitial fluid from the literature is 2.0 S/m,[8] which is similar to that of blood serum (1.7 S/m)[30] and cerebrospinal fluid (1.8 S/m).[2] The conductivity of the extracellular fluid based on chemical composition is also on the order of 2.0 S/m.[32] We used the latter value of 2.0 S/m

as the conductivity of the extracellular electrolyte and for the blood plasma. Assuming that the same fluid filled the pores that made up 1% of the capillary wall, we estimated the effective conductivity of the capillary wall to be of the order of 0.02 S/m.

The histology of the ICS is quite complex, as the interior of a myocyte is not just a homogeneous isotropic electrolyte, myofibrils and mitochondria are stacked along the fiber direction of the myocardium. As the myofibrils and mitochondria are less conducting than the surrounding electrolyte,[5,23] they form a different barrier for currents traveling along the fiber direction than for the currents perpendicular to this direction. Hence, the conductivity of the intracellular space of a myocyte must be anisotropic. Schaper *et al.*[29] measured a volume fraction occupied by the myofibrils of 62%, by the mitochondria of 23%, and by "empty" space of 15%. Assuming that about 60% of the myofibrils take part in the conduction process[5] and that the mitochondria are not conducting at all,[23] we derived a volume fraction of the conducting electrolyte of about 50%. Assuming that the stacks of mitochondria and the myofibrils can be described by cylinders aligned along the fiber axis, the effective cellular conductivity is a suspension of non-conducting cylinders in a conducting media. For such a suspension the anisotropy factor is about 2, and the effective conductivity along the fiber direction can be computed by multiplying the conductivity of the cytoplasmic fluid with its volume fraction.[24]

The conductivity of the cytoplasmic fluid depends primarily on potassium ions and can be estimated from the potassium concentration and the diffusion constant of potassium in the intracellular space. Kushmerick and Podolsky[19] measured the diffusion coefficient of potassium in the cytoplasm of frog muscle as 55% of the diffusion coefficient of potassium in water. Assuming an intracellular potassium concentration of 140 mM, an ion specific conductivity of 91×10^{-4} m^2 S/mol and a decrease of the ionic mobility by a factor 2, one can derive a cytosolic conductivity of 0.7 S/m and an effective myocyte conductivity in the range of 0.3 S/m along the fiber direction and 0.15 S/m across. Brown *et al.*[4] measured the effective conductivity of the cytoplasm along the long axis of myocytes and found a value of 0.17 S/m at room temperature; correcting this value to body temperature, one derives a value of about 0.23 S/m, which is in reasonable agreement with the value of 0.3 S/m derived earlier. In the model we assumed a conductivity of 0.3 S/m in the longitudinal and 0.15 S/m in the transverse direction.

Measurements performed on isolated rat myocyte pairs have indicated the cell-to-cell resistance to be about 2 MΩ,[21,35] the latter being a combination of the gap junction resistance and the resistance of the cytoplasm.[36] As argued by Metzger *et al.*[21] most isolated cell pairs were not pure end-to-end coupled myocytes but they had a side-to-side coupling as well and not all processes were coupled to the other myocyte. Assuming that the cell-to-cell resistance was measured starting from the center of one myocyte to the center of the next one and that the conductivity of the cytoplasm is 0.3 S/m the access resistance would be about 1 MΩ, which leaves another approximately 1 MΩ for the gap junctions themselves. To compute the effective surface resistance used to model the conduction through the gap junctions, we assumed that the value of 1 MΩ was spread out over half of the cross section of an average myocyte.

TABLE 1. Overview of the parameters used in the conductivity model.

Parameter	Value
Cytoplasm longitudinal conductivity	0.3 S/m
Cytoplasm transverse conductivity	0.15 S/m
Interstitial conductivity	2.0 S/m
Capillary wall conductivity	0.02 S/m
Blood plasma conductivity	2.0 S/m
Haematocrit	50%
Gap-junction resistivity	1.45×10^{-4} Ωm^2
Cell membrane resistivity	$+\infty$ Ωm^2
Average cell cross-section	300 μm^2
Average cell length	95 μm
Volume fraction myocytes	84%
Volume fraction interstitial space	11%
Volume fraction capillaries	5%

Table 1 contains an overview of all the different parameters chosen for the model.

RESULTS

Figure 4 shows effective intracellular conductivity as a function of the various geometrical parameters. The bottom graph of each column shows in detail the influence of the gap junction resistance on conductivity.

The relative sizes of the local variation in the geometry mainly affects the transverse effective conductivity. Hence, the model predicts that, on the scale of the model (a cluster of $4 \times 4 \times 4$ myocytes), one can expect a considerable variation in the transverse effective intracellular conductivity.

The figure shows that the anisotropy factor depends considerably on the values chosen for average myocyte length and myocyte cross section. The ranges chosen for these parameters depict the lowest and highest values found in the literature and can change the anisotropy factor by at least a factor of 2.

Figure 5 contains the results from the same variations in myocyte length and cross section for the extracellular space. In contrast to the intracellular space conductivities, the extracellular conductivities show a far smaller dependence on the size of the myocytes. In these simulations, despite the variations in myocyte size, the extracellular volume fraction was kept more or less constant.[10] The latter situation, for instance, corresponds to the observations made by Gerdes and Kasten,[10] who found significant changes in myocyte

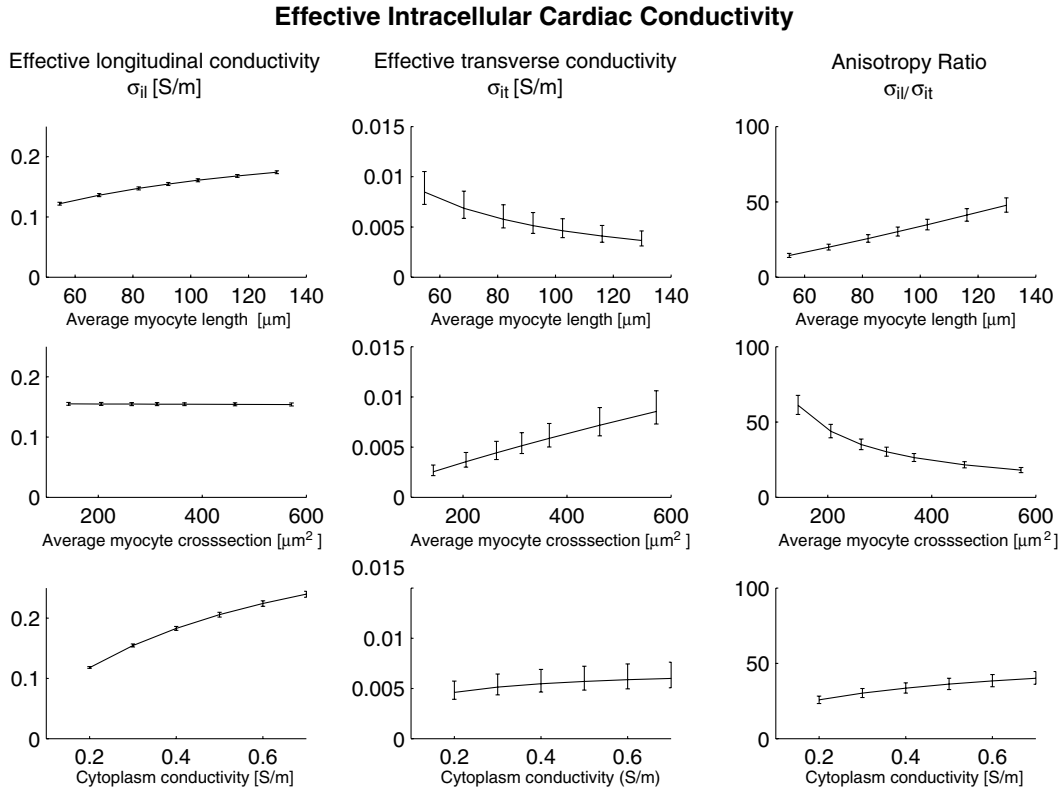

FIGURE 4. Effective intracellular conductivity as a function of the average myocyte length, average myocyte cross section, and cytoplasm conductivity. The first column displays the longitudinal effective conductivity, the second the effective transverse conductivity, and the third the anisotropy ratio. In each of the graphs only one parameter is varied, the other parameters are kept at the following reference values: 95 μm for the average myocyte length, 300 μm^2 for the average myocyte cross section, and 0.3 S/m for the effective cytoplasm conductivity. The conductivity values shown, represent an average value over 10 simulations in which the shape of the myocytes is altered while maintaining the average length and cross section of the myocytes in the model. The error bars indicate the maximum and minimum values found for the effective conductivities. Note that the error bars for the longitudinal case are tiny. All values depicted were computed by applying a potential difference over the simulated tissue and calculating the total amount of current flowing in respectively the intracellular and extracellular space.

sizes between epicardium and endocardium, but no changes in the volume fraction of the ECS.

We did not simulate the response of ECS conductivity to interstitial electrolyte conductivity under the assumption that its effect on bulk conductivity would be linear.

Using the parameters in Table 1 we computed an effective intracellular conductivity of about 0.16 S/m (longitudinal) and 0.005 S/m (transverse), and an effective extracellular conductivity of about 0.21 S/m (longitudinal) and 0.05 S/m (transverse).

In a separate study, we examined the effect of the capillaries through two simulations: (1) a full capillary model that included a capillary wall, blood plasma, and red blood cells, and (2) a model in which the space of the capillaries was assumed to be non-conducting, i.e., the conductivity was set to zero. The effective conductivity values from both models differed no more than 10% and the capillary space for both the longitudinal and transverse currents acted as a poor conductor (in comparison to the interstitial space).

DISCUSSION

One advantage of simulations such as ours is that they allow predictions over a wider range of parameters than might be possible using only experiments. For such predictions to be valid, however, the model must also produce results that compare to those experimental measurements that are available. For parameters in the middle of the range we tested, we computed effective intracellular conductivity of approximately 0.16 S/m (longitudinal) and 0.005 S/m (transverse), and an effective extracellular conductivity of about 0.21 S/m (longitudinal) and 0.05 S/m (transverse). The bulk conductivity (overall conductivity of both the intracellular and extracellular volume) thence should be of the order $0.16 + 0.22 \approx 0.38$ S/m (longitudinal) and $0.05 + 0.005 \approx 0.05$ S/m (transverse) with an anisotropy ratio of about 7. By comparison, Gabriel *et al.*[9] measured a bulk longitudinal conductivity of about 0.35 S/m, which is close to the value found using our geometrical model.

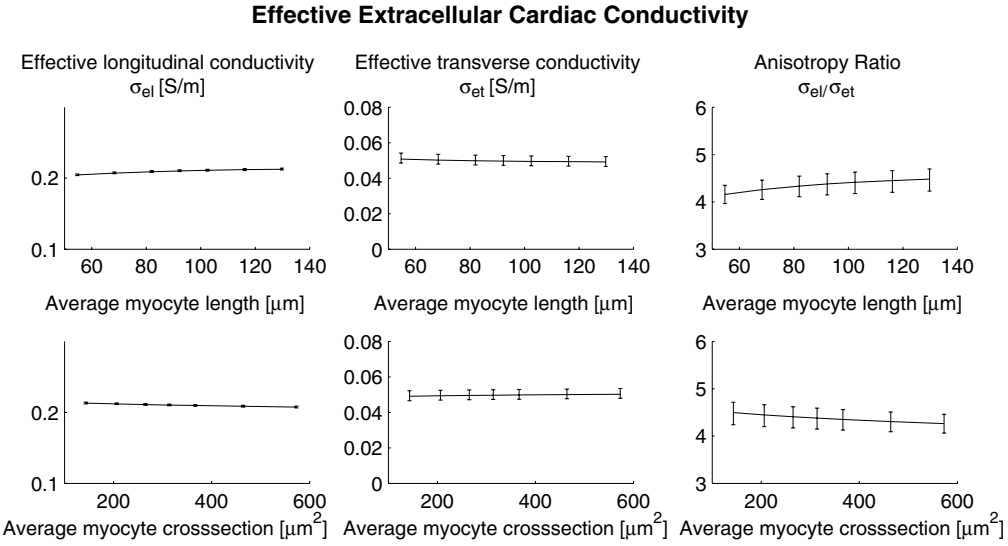

FIGURE 5. Effective extracellular longitudinal and transverse conductivity as a function of changes in average myocyte length and average myocyte cross section. In each of the graphs only one parameter is varied. The other parameters are kept at reference values: 95 μm for the average myocyte length and 300 μm^2 for the average myocyte cross section. The extracellular fluid conductivity was assumed to be 2 S/m. The conductivity values shown, represent an average value over 10 simulations in which the shape of the myocytes is altered while maintaining the average length and cross section of the myocytes in the model. The error bars indicate the maximum and minimum values found for the effective conductivities.

The results of the model for extracellular conductivity agreed more closely with reported estimates from the literature than the intracellular conductivity. In particular, the values of Roberts and Scher[27,28] of 0.22 and 0.13 S/m were in the range of the values we found for the extracellular longitudinal conductivity (0.20–0.23 S/m) and the extracellular anisotropy factor (4–5), respectively. However, the value of 0.62 S/m reported by Clerc[7] for the longitudinal extracellular conductivity seems rather high. If we assume that the extracellular volume fraction is no more than 20%, that the extracellular space is not blocked in the longitudinal direction, and that the vasculature does not play a substantial role in conducting current, Clerc's value would imply an interstitial fluid conductivity of about $0.62/0.2 \approx 3.0$ S/m, which, in turn, would imply that the sodium or chloride concentrations in the interstitial fluids were larger than physiological values. In other words, Clerc's estimate is difficult to justify under any reasonable range of parameter values. The intracellular conductivity is slightly lower than the values reported in literature, although the average value of 0.16 S/m is close to the value found by Clerc[7] (0.17 S/m) and Le Guyader *et al.*[20] (0.20 S/m).

The only conductivity that was hard to match to literature values was the intracellular transverse conductivity of about 0.005 S/m. This conductivity is significantly lower than values found in literature, see Table 1. Possible explanations for this mismatch include the following: (1) the resistance of the gap junctions is lower than we estimated even though our estimation is already in the lower range of literature values; and (2) the distribution of gap junctions is far more homogenous than estimated and not mostly confined to the ends of the myocytes as antibody staining suggests.

A further advantage of using simulations is that it offers a vehicle to explain some of the discrepancies that exist in the values reported from experiments. In the case of myocardial tissue conductivity, there are indeed substantial differences in the literature that warrant explanation and resolution because these values are crucial components of computations of cardiac bioelectric fields. Experimental determination of conductivity is challenging and estimates in the literature vary widely, in part because of differences in species, in the experimental preparations (*in vivo vs. in vitro*), in the level of perfusion, and in the models used to interpret the data. Table 2 gives an overview of the values found in the literature for the bidomain conductivities, with the first three references providing the values most commonly used in whole-heart models.

At least one other group has taken a modeling approach to estimate the four bidomain conductivities based on an assumed tissue geometry and a hexagonal grid of myocardial cells with three gap junctions located at each end of each cell.[22] The resulting estimates of three of the four bidomain conductivities, σ_{il}, σ_{el}, and σ_{et}, were within the (wide) ranges of the literature values. The estimate of the transverse intracellular conductivity (σ_{it} however, was orders of magnitude smaller than any other value in the literature.

Our model predicts that the anisotropy of conductivity is far larger in the intracellular space than the extracellular

TABLE 2. Conductivity values (S/m) in the literature.

Reference	σ_{il}	σ_{it}	σ_{el}	σ_{et}	$\frac{\sigma_{il}}{\sigma_{el}}$	σ_{l}	σ_{t}
Clerc[7]	0.17	0.019	0.62	0.24	0.27	0.8	0.26
Roberts[27]	0.28	0.026	0.22	0.13	1.27	0.55	0.15
Roberts[28]	0.34	0.06	0.12	0.08	2.83	0.47	0.14
Kleber[18]	0.45		0.4		1.1	0.86	
Tsai[34]						0.29	0.33
Cascio[6] *	0.31		0.39			0.70	
LeGuyader[20]	0.20	0.024	0.3	1.74			

*Calculated from total resistance and ratio between intra and extracellular resistance.

space. Similarly, our model also predicts that the anisotropy of the bulk conductivity is larger than the value derived by applying cable theory to measurements of propagation velocity.[7,28] The model suggests that the major determinant of intracellular anisotropy is the distribution of gap junctions; when gap junctions are more or less confined to the ends of the myocytes (where the literature suggests they are located[3,16,31]), the transverse currents have to pass through far more gap junctions than the longitudinal currents in order to travel a given distance along a straight line. In order to have a lower anisotropy ratio for the intracellular space than is predicted by our model, which some of the literature suggests, the number of transverse gap junctions must be far larger than in our model. Another way to obtain a smaller anisotropy value, is a higher intracellular resistance and a lower gap junction resistance, or a lower intracellular anisotropy. Although the estimated intracellular anisotropy may be lower, as the myofibrils and mitochondria do not line up perfectly in cylinders and hence the model assuming non-conducting cylinders in an inhomogeneous medium may overestimate the conductivity along the fibers and underestimate the conductivity across the fibers. However, the difference in global anisotropy ratio will not change much, as the gap junctions are the main resistive contribution to the resistance in the direction across the fiber. Hence, a lower conductivity of the cytoplasm and a higher conductivity of the gap junctions is a more likely explanation, this would, however, indicate a lower mobility of potassium in the cytoplasm itself and to lower apparent conductivities of the cytoplasm than reported in literature.[4]

A further finding that has implications for the creation of models of myocardium is that small-scale randomization (each cluster of myocytes for which we computed conductivities had slightly differently shaped myocytes) proved to have only a small impact on the effective conductivity. The effect of this variation was an 11% deviation from the mean for the effective transverse conductivity (intracellular or extracellular) and less than 5% deviation for effective longitudinal conductivity. We note that the latter value is probably an underestimation of the variation in real tissue, as all the capillaries in the model ran perfectly parallel to the fiber direction, whereas in reality there are always capillary cross connections. In contrast, the more global geometrical and resistivity parameters, such as the average myocyte length, the average myocyte cross section, and the gap junction resistivity, had a far larger impact on the effective conductivity than did random variation of these parameters over the same ranges about a given average value. One has to point out that the size of the simulated cluster of myocytes influences the local variation in the effective conductivity; as the cluster size increases, the differences in transverse conductivity between clusters will decrease, since the transverse conductivity variations will tend to average out over larger distances.

Although the geometrical model we developed bore many similarities to realistic tissue, there were still many simplifications needed. The model assumed a regular grid of myocytes, albeit with local perturbations, which forces current in any transverse direction to flow through approximately the same number of cells. It is unclear from histology, however, whether this assumption is likely to skew our values. Another simplification we made was to make the sheet of interstitial fluid between cells of the same thickness everywhere. A more realistic model would allow for random fluctuations, however, there is little data available upon which to determine realistic values for such perturbation. A similar randomization of the gap junction resistance is another parameter we would like to add in future simulations. Another simplification is that we modeled the membrane as non-conducting, in reality, the membrane resistance is high but not infinite, and currents will cross over from the intracellular domain into the extracellular domain and back. As the simulations presented were focused on generating values for the bidomain approximation, we chose to leave out the membrane altogether.

In summary, a model of the conductivity of cardiac tissue can be instrumental in understanding how the conductivity relates to the structure of cardiac tissue. Moreover, this modeling approach can serve as a starting point for a multiscale model of the heart in which changes in physiology, e.g. ischemia, are reflected in the bidomain conductivities used in a full-size model of the myocardium, an example of which, we have already developed.[14]

REFERENCES

[1] Anversa, P., A. V. Loud, F. Giacomelli, and J. Wiener. Absolute morphometric study of myocardial hypertrophy in experimental hypertension, II. infrastructure of myocytes and interstitium. *Lab. Invest.* 38(5):597–609, 1978.

[2] Baumann, S. B., D. R. Wozny, S. K. Kelly, and F. M. Meno. The electrical conductivity of human cerebrospinal fluid at body temperature. *IEEE Trans. Biomed. Eng.* 44:220–223, 1997.

[3] Beardslee, M. A., L. D. Lerner, P. N. Tadros, J. G. Laing, E. C. Beyer, K. A. Yamada, A. G. Kleber, R. B. Schuessler, and J. E. Saffitz. Dephosphyorylation and intracellular redistribution

of ventricular Connexin43 during electrical uncoupling induced by ischemia. *Circ. Res.* 87:656–662, 2000.
[4]Brown, A. M., K. S. Lee, and T. Powell. Voltage clamp and internal perfusion of single rat heart muscle cells. *J. Physiol.* 318:455–477, 1981.
[5]Caille, J. P. Myoplasmic impedance of the barnacle muscle fiber. *Can. J. PhysioL Pharmacol.* 53(6):1178–1185, 1975.
[6]Cascio, W. E., H. Yang, T. A. Johnson, B. J. Muller-Borer, and J. J. Lemasters. Electrical properties and conduction in perfused papillary muscle. *Circ. Res.* 89:807–814, 2001.
[7]Clerc L. Directional differences of impulse spread in trabecular muscle from mammalian heart. *J. Physiol.* 255:335–346, 1976.
[8]Foster, K. R., and H. P. Schwan. Dielectric properties of tissues and biological materials: A critical review. *Crit. Rev. Biomed. Eng.* 17(1):25–104, 1989.
[9]Gabriel, S., R. W. Lau, and C. Gabriel. The dielectric properties of biological tissues. II. Measurements in the frequency range 10–20 GHz. *Phys. Med. Biol.* 41:2251–2269, 1996.
[10]Gerdes, A. M., and F. H. Kasten. Morphometric study of endomyocardium and epimyocardium of the left ventricle in adult dogs. *Am. J. Anal.* 159(4):389–394, 1980.
[11]Gerdes, A. M., S. E. Kellerman, J. A. Moore, K. E. Muffly, L. C. Clarck, P. Y. Reaves, K. B. Malec, P. P. McKeown, and D. D. Schocken. Structural remodeling of cardiac myoctes in patients with ischemic cardiomyopathy. *Circulation* 86:426–430, 1992.
[12]Henriquez, C. S. Simulating the electrical behavior of cardiac tissue using the bidomain model. *Crit. Rev. Biomed. Eng.* 21(1):1–77, 1993.
[13]Hooks, D. A., K. A. Tomlinson, S. G. Marsden, I. J. LeGrice, B. H. Smaill, A. J. Pullan, and P. J. Hunter. Cardiac microstructure: Implications for electrical propagation and defibrillation in the heart. *Circ. Res.* 91:331–338, 2002.
[14]Hopenfeld, B., J. G. Stinstra, and R. S. MacLeod. Mechanism for ST depression associated with contiguous subendocardial ischemia. *Journal Cardiovascular Electrophysiology* 15(10):1200–1206, 2004.
[15]Hopenfeld, B., J. G. Stinstra, and R. S. MacLeod. The effect of conductivity on ST segment epicardial potentials arising from subnedocardial ischemia. *Ann. Biomed. Eng.* 33(6):751–763, 2005.
[16]Jain, S. K., R. B. Schuessler, and J. E. Saffitz. Mechanisms of delayed electrical uncoupling induced by ischemic preconditioning. *Circ. Res.* 92(10):1138–1144, 2003.
[17]Johnston, P. R., and D. Kilpatrick. The effect of conductivity values on ST segment shift in Subendocardial ischaemia. *IEEE Trans. Biomed. Eng.* 50(2):150–158, 2003.
[18]Kleber, A. G., and C. B. Riegger. Electrical constants of arterially perfused rabbit papillary muscle. *J. Physiol.* 385:307–324, 1987.
[19]Kushmerick, M. J., and R. J. Podolsky. Ionic mobility in muscle cells. *Science* 166:1297–1298, 1969.
[20]LeGuyader, P., P. Savard, and F. Trelles. Measurement of myocardial conductivities with an eight-electrode technique in the frequeny domain. In Proceeding 17th Annual Conference of the IEEE Engineering in Medicine and Biology Society. Montreal, Canada, 1995.
[21]Metzger, P., and R. Weingart. Electric current flow in ell pairs isolated from adult rat hearts. *J. Physiol.* 366:177–195, 1985.
[22]Neu, J. C., and W. Krassowska. Homogenization of syncytial tissues. *Crit. Rev. Biomed. Eng.* 21:137–199, 1993.
[23]Pauly, H., L. Packer, and H. P. Schwan. Electrical properties of mitochondrial membranes. *J. Biophys. Biochem. Cytol.* 7(4):589–601, 1960.
[24]Peters, M. J., J. G. Stinstra, and M. Hendriks. Estimation of the electrical conductivity of human tissue. *Electromagnetics* 21:545–557, 2001.
[25]Plonsey, R. *Bioelectric Phenomena*. New York: McGraw Hill, 1969.
[26]Poole-Wilson, P. A. The dimensions of human cardiac myocytes; confusion caused by methodology and pathology. *J. Moll. Cell. Cardiol.* 27:863–865, 1995.
[27]Roberts, D. E., L. T. Hersch, and A. M. Scher. Influence of cardiac fiber orientation on wavefront voltage, conduction velocity and tissue resistivity. *Circ. Res.* 44:701–712, 1979.
[28]Roberts, D. E., and A. M. Scher. Effect of tissue anisotropy on extracellualar potential fields in canine myocardium in situ. *Circ. Res.* 50:342–351, 1982.
[29]Schaper, J., E. Meiser, and G. Stammler. Ultrastructural morphometric analysis of myocardium from dogs, rats, hamsters, mice, and from human hearts. *Circ. Res.* 56(3):377–391, 1985.
[30]Schwann, H. P., and C. F. Kay. The conductivity of living tissues. *Ann. N.Y. Acad. Set* 65:1007–1013, 1956.
[31]Spach, M. S., J. F. Heidlage, P. C. Dolber, and R. C. Barr. Electrophysiological effects of remodelling cardiac gap junctions and cell size: Experimental and model studies of normal cardiac growth. *Circ. Res.* 86, 2000.
[32]Stinstra, J. G., and M. J. Peters. The influence of fetoabdominal tissues on fetal ECGs and MCGs. *Arch. Physiol. Biochem.* 110(3): 165–176, 2002.
[33]Trautman, E. D., and R. S. Newbower. A practical analysis of the electrical conductivity of blood. *IEEE Trans. Biomed. Eng.* 30(3):141–153, 1983.
[34]Tsai, J.-Z., J. A. Will, S. Hubbard-Van Stelle, H. Cao, S. Tungjitkusolmun, Y. B. Choy, D. Haemmerich, V. R. Vorperian, and J. G. Webster. Error analysis of tissue resistivity measurement. *IEEE Trans. Biomed. Eng.* 49:472–483, 2002.
[35]Weingart, R. Electrical properties of the nexal membrane studied in rat ventricular cell pairs. *J. Physiol.* 370:267–284, 1986.
[36]Wilders, R., and H. J. Jongsma. Limitations of the dual voltage clamp method in assaying conductance and kinetics of gap junction channals. *Biophys. J.* 63:942–953, 1992.